Revista Mexicana de Astronomía y Astrofísica, **57**, 67–80 (2021)

https://doi.org/10.22201/ia.01851101p.2021.57.01.04

SPECKLE INTERFEROMETRY AT THE OBSERVATORIO ASTRONÓMICO NACIONAL. VII

V. G. Orlov

Instituto de Astronomía, Universidad Nacional Autónoma de México, Ciudad de México, México.

Received August 25 2020; accepted September 22 2020

ABSTRACT

The results of speckle interferometric measurements of binary stars performed during June, 2016 with the 2.1 m telescope at the Observatorio Astronómico Nacional at SPM (México) are given. We report 480 astrometric measurements of 468 double stars systems. The measured angular separations ρ range from $0''.091$ to $5''.93$. Most of the observed pairs (414 out of 468) are close double stars having separations of $\rho \leq 1''$. We confirm as double stars 59 targets and we found 3 new pairs with separation of less than $1''$. Finally, we show that the high resolution autocorrelation function in polar coordinates allows to easily recover astrometric parameters even in the presence of strong telescope aberrations.

RESUMEN

Se presentan las mediciones de interferometría de motas de estrellas binarias, realizadas durante el mes de junio de 2016 con el telescopio de 2.1 m del Observatorio Astronómico Nacional en SPM (México). Reportamos 480 mediciones astrométricas de 468 sistemas de estrellas dobles. Las separaciones angulares medidas ρ van desde $0''.091$ a $5''.93$. La mayoría de los pares observados (414 de 468) son estrellas dobles cercanas con una separación $\rho \leq 1''$. Confirmamos 59 objetos como estrellas dobles e identificamos 3 nuevos pares con una separación de menos de $1''$. Finalmente, mostramos que la función de autocorrelación de alta resolución en coordenadas polares permite recuperar fácilmente los parámetros astrométricos, incluso en presencia de fuertes aberraciones del telescopio.

Key Words: binaries: close — techniques:high angular resolution — techniques: interferometric

1. INTRODUCTION

In this paper we report astrometric results for double stars obtained by speckle interferometric observations carried out with the 2.1 m telescope of Sierra San Pedro Mártir National Astronomical Observatory (OAN-SPM) in June of 2016. This is the seventh in a series of publications that started with speckle interferometric measurements performed with the OAN telescopes in 2008 (Orlov et al. 2009). As in our previous publications, we focus on double stars from the Washington Double Star (WDS) catalog (Worley & Douglass 1997).

The Speckle Interferometry (SI) (Labeyrie 1970) is one of the most used high resolution techniques. This method allows the observer to obtain information about relative positions in close binary stars systems with diffraction-limited accuracy. This technique was most widely used in the study of binary and multiple stars (Tokovinin et al. 2020; Guerrero et al. 2020; Mitrofanova et al. 2020). The observation methodology and data processing of SI is very well studied and described by Tokovinin et al. (2010).

The 2.1 m telescope of OAN-SPM has a thin primary mirror; its shape is corrected by air bags. The process of correction takes about one hour and is performed only once before observations. During the night, the temperature of the primary mirror and of the telescope mount change, which leads to thermal deformations. Also, corrections introduced by the airbags depend on the hour angle and the zenith distance of the target. As a result, we have different aberrations for each object (Figure 1). Because of this, it is unfeasible to construct a universal synthetic speckle interferometric transfer function or even to

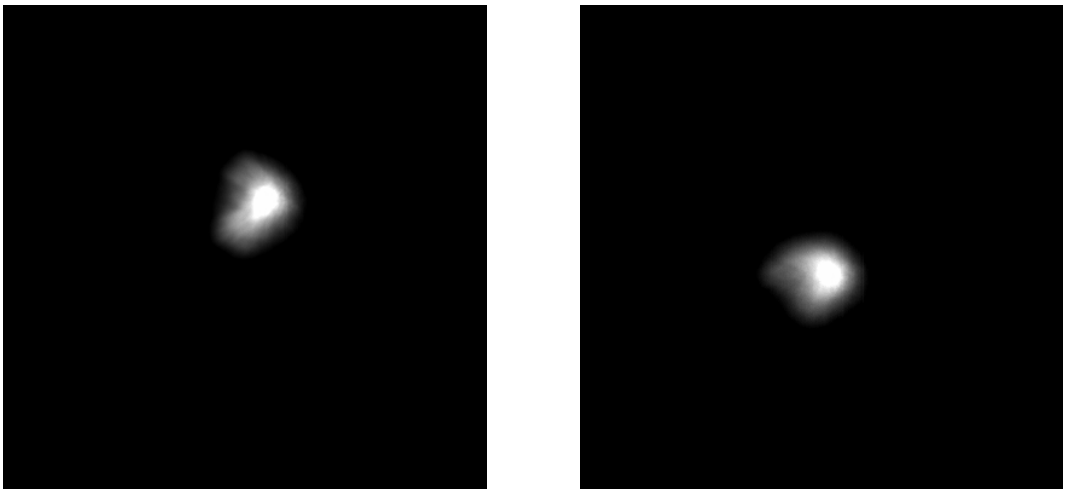

(a) (b)

Fig. 1. Long exposure image of WDS 20480+3917 (a). Long exposure image of WDS 18003+2154 (b). Both images show very strong coma aberration with different angles.

use a reference star. This fact limits the possibility of finding both astrometric and photometric parameters of double stars. In addition, the telescope's vibration distorts the specklegrams. All these factors have a greater impact on the ability to recover photometric parameters than on the recovery of astrometric parameters. Therefore, in this study we focus on improving the recovery of astrometric parameters.

In order to estimate astrometric parameters, we designed an algorithm which allows one to recover each measurement from the distorted power spectrum. In section 3.2 we describe the calculation of the high resolution autocorrelation function in polar coordinates. This algorithm allows for blind searching of the astrometric parameters ρ and θ of double stars, since it finds the coordinates of the absolute maximum of a two-dimensional discrete function.

2. OBSERVATIONS

Speckle interferograms were taken during four nights in the summer of 2016, from June 28 to July 1 at the 2.1 m telescope of the Observatorio Astronómico Nacional (OAN), which is located at the astronomical site Sierra San Pedro Mártir, México.

The observations were performed using the EMCCD iXon Ultra 888 from Andor Technology. This is a low-noise, high-sensitivity EMCCD camera that can be cooled thermoelectrically down to $-95°C$ which provides excellent elimination of dark noise, even for the short time exposures. The detector has quantum efficiency higher than 80% in the range of $450 - 750\ nm$, with a maximum of 95% at 550 nm (V-band). This camera allows a fast frame rate so it can be used for speckle interferometry. The detector has 1024×1024 square pixels of 13 μm per side.

The observations were carried out using broadband filters V(538/98 nm), R(630/118 nm) and I(894/330 nm) from the Johnson-Cousins set. The size of the diffraction-limited speckle (λ/D) for the 2.1m telescope is approximately 70 mas at this filter wavelength. Given these parameters, we need an angular pixel scale of about 35 mas to obtain a Nyquist sampling of specklegrams. To provide a suitable sampling, we used the $f/7.5$ secondary mirror combined with a microscope objective lens $\times 4$.

We recorded 500 speckle frames of 400×400 pixel per object, taken with exposure times of 29.5 ms. We use EM gain of 1/300 photons/e^- for all observations.

The seeing was better than $1''$over all the observing nights. However, aberrations introduced by the telescope have a larger effect (Figure 1). As a result, long exposure images have a resolution of about $1.5''$.

3. DATA PROCESSING

The first step of the data processing is the dark field correction of detected images $I'_n(\mathbf{x})$:

$$I_n(\mathbf{x}) = I'_n(\mathbf{x}) - Dark(\mathbf{x}), \tag{1}$$

where $\mathbf{x}$ is a 2D spatial coordinate, $I_n(\mathbf{x})$ is the corrected image, $Dark(\mathbf{x})$ is the average dark image captured with a closed shutter (Figure 2 left). In order to remove the reading noise, we also set to zero all values less than 4σ of dark (Figure 2 right).

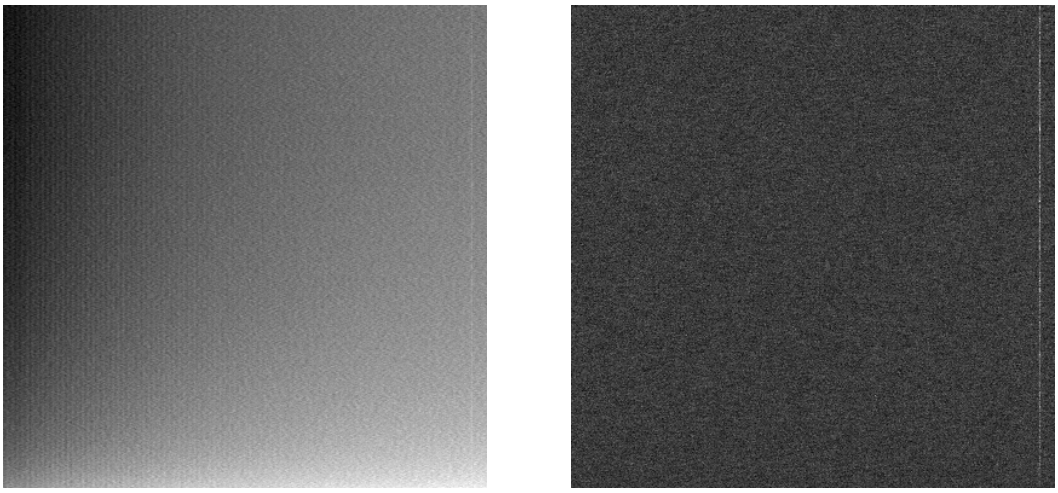

Fig. 2. The average Dark image (left) and σ of Dark image (right).

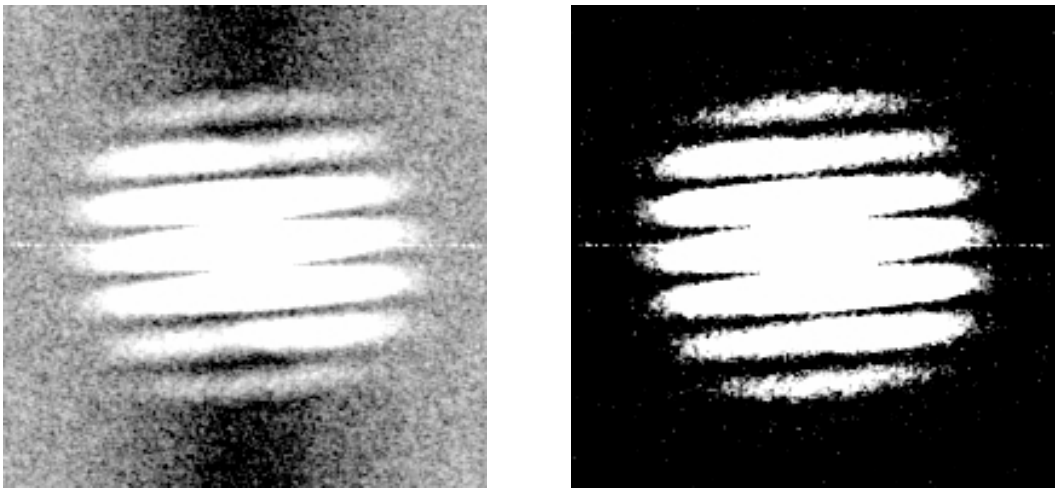

Fig. 3. Power spectrum of WDS 20312+1116 before photon bias correction (left) and after correction (right). The separation is 0.″3.

3.1. *Unshifted Power Spectrum*

The next step is to calculate the averaged power spectrum (PS) for each star:

$$PS(\mathbf{f}) = \left\langle \left| FT\left\{ I_n(\mathbf{x}) \right\} \right|^2 \right\rangle , \tag{2}$$

where $\mathbf{f}$ is a spatial frequency, $FT\{...\}$ is the Fourier transform and $\langle ... \rangle$ denotes averaging over all images.

In the case of low light images, the averaged power spectrum can be expressed as (Kerp et al. 1992):

$$PS(\mathbf{f}) = P(\mathbf{f}) \cdot \left| G(\mathbf{f}) \right|^2 + q \left| G(\mathbf{f}) \right|^2 , \tag{3}$$

where $P(\mathbf{f})$ is the unshifted estimation of the power spectrum, q is some constant, $\left|G(\mathbf{f})\right|^2$ is the power spectrum of the photon event shape function, also known as photon bias. The photon bias $\left|G(\mathbf{f})\right|^2$ can be determined as the normalized power spectrum of the night sky. $\left|G(\mathbf{f})\right|^2$ is constant in the Y direction for this camera. Thus, it can be determined directly from $PS(\mathbf{f})$ (Figure 3, left) by analysis of its part beyond the cut-off frequency of telescope. The unshifted power spectrum of specklegrams $P(\mathbf{f})$ is shown in Figure 3 (right). Therefore, it can be presented as:

$$P(\mathbf{f}) = \left| O(\mathbf{f}) \right|^2 \left\langle \left| S_n(\mathbf{f}) \right|^2 \right\rangle , \tag{4}$$

where $\left|O(\mathbf{f})\right|^2$ is the power spectrum of the object, and $\left\langle \left| S_n(\mathbf{f}) \right|^2 \right\rangle$ is the speckle interferometric transfer

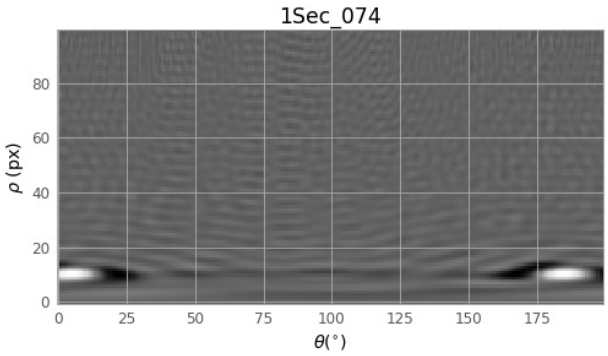

Fig. 4. The ACF in polar coordinates for WDS 20312+1116. The separation is 0.″3.

function. The speckle interferometric transfer function can be obtained by observing a reference star, or one can construct a universal synthetic speckle interferometric transfer function (Tokovinin et al. 2010). If one needs only astrometric parameters, they can be obtained without the speckle interferometric transfer function, directly from P(**f**).

3.2. *Autocorrelation Function in Polar Coordinates*

In order to find astrometric parameters from the unshifted power spectrum we calculated the high resolution autocorrelation function in polar coordinates ACF_p:

$$ACF_p(\rho,\theta) = const \int_0^{\infty}\int_0^{2\pi} \cos(2\pi r\rho\cos(\theta-\phi))\times \times P(r,\phi)W(r,\phi)rdrd\phi, \quad (5)$$

where $W(r,\phi)$ is the window which excludes part of $P(r,\phi)$ beyond the cut-off frequency of the telescope f_T and for frequencies lower than the atmospheric cutoff f_A. Also, taking in to account central symmetry of $P(r,\phi)$ equation 5 can be rewritten as:

$$ACF_p(\rho,\theta) = const \int_{f_A}^{f_T}\int_0^{\pi} \cos(2\pi r\rho\cos(\theta-\phi))\times \times P(r,\phi)rdrd\phi. \quad (6)$$

One example of ACF_p is shown in Figure 4. The position of the maximum gives us ρ and θ which determine the position of the component in the coordinates of the detector.

Now let us see if ACF_p allows us to find astrometric parameters when the power spectrum is distorted by vibrations and strong aberrations of the telescope. As shown in Figure 5 (left) the power spectrum loses the high frequencies in the vertical direction. However, the high resolution ACF_p has a strong maximum (Figure 5, right). The precision of determining astrometric parameters of the binary system depends on the accuracy with which we can determine the coordinates of the maximum of the discrete function ACF_p. Thus, we can recover the astrometric parameters from the distorted power spectrum. Although measurements can be carried out without the speckle interferometric transfer function correction, its use improves their accuracy.

3.3. *180 Degree Ambiguity*

The power spectrum has a 180° ambiguity. To deal with this issue, we used the self-calibrating shift-and-add technique (Christou et al. 1986). The technique allows us to get diffraction-limited images without using any reference star. When the components have similar magnitudes, the result of this technique is similar to the diffraction-limited autocorrelation, as in Figure 6 (left), contrary to the case in which there is a clear difference between the components, as shown in Figure 6 (right). This double star has a difference of one magnitude between components. This technique allows us to overcome the common 180 degree ambiguity, thus obtaining a reconstruction of the close double star system. Then we can obtain the real θ (position angle) and ρ (separation) by calibration.

3.4. *Calibration*

To perform the calibration, we need to find the pixel scale and the position angle offset. There are two common ways to do this. The first one is by observing some binary stars which have known orbits of grade 1 and calculating ephemerides from the orbital elements. The second way is by observing double stars with very slow relative motion of the components. In this case, ephemerides are calculated by linear approximation of the component motion, or by using the last known value of ρ and θ if there is no evidence of motion over more than 20 years. Most suitable for this method are optical doubles with slow proper motion. This method is preferable to the first one, because the accuracy of speckle interferometric measurements with 2-meter telescopes exceeds the accuracy of even the best orbits (Tokovinin et al. 2015).

For the astrometric calibration, we selected 21 systems with a separation ranging from 4″to 6″ which had more than one reliable observation from the Fourth Catalog of Interferometric Measurements

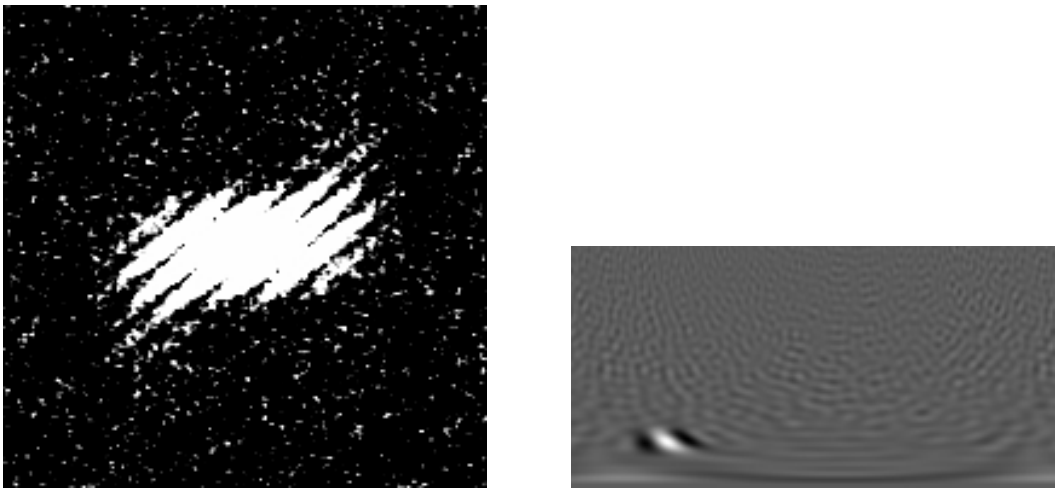

Fig. 5. Power spectrum $P(\mathbf{f})$ of WDS 14394-0733 distorted by vibrations and aberrations of the telescope (left). ACF_p of WDS 14394-0733 obtained from its $P(\mathbf{f})$ (right). The separation is 0.″55.

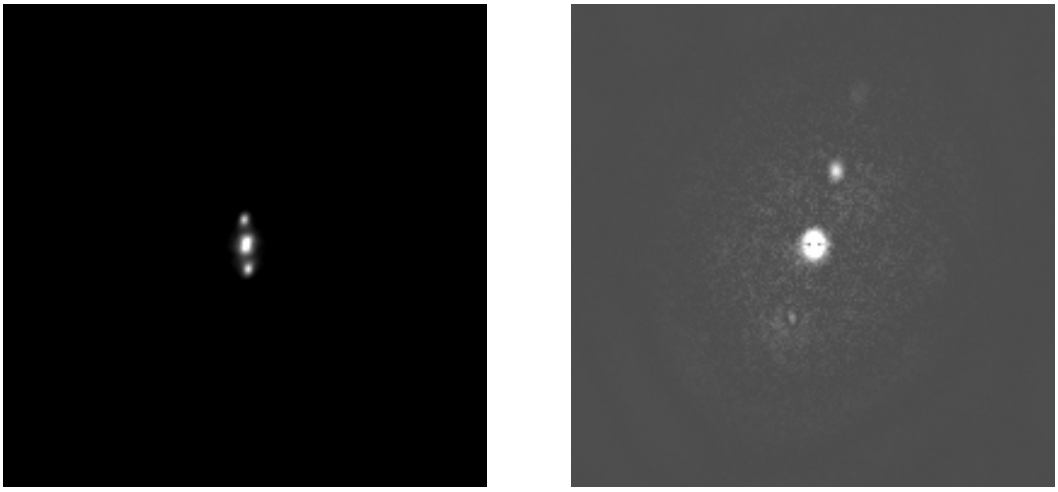

Fig. 6. Example of the reconstruction of WDS 20312+1116 (left) and WDS 19326+0435, $\Delta m = 1$(right).

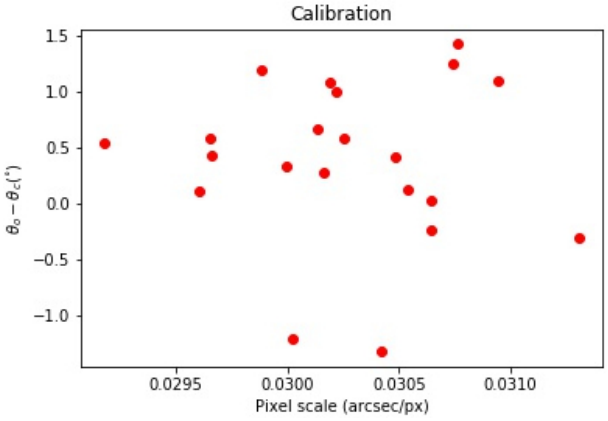

Fig. 7. Calibration.

of Binary Stars (Hartkopf et al. 2001) and from the WDS catalog. These 21 systems also have very slow movements and a long time base of observations. A comparison with our data (Figure 7) gives us the following offset for the position angle $\theta_0 = -0.42° \pm 0.14°$ and a pixel scale $s = 0''.03026 \pm 0''.00009$ per pixel.

4. ASTROMETRIC MEASUREMENTS

The astrometric measurements we obtained for double stars are displayed in four tables (Tables 1-4). Table 1 presents astrometric measurements of 21 double stars used for calibration. All these systems show slow motions of components. The first column contains the epoch-2000 coordinates in the

TABLE 1

WIDE DOUBLE STARS WITH VERY SLOW RELATIVE MOTION

WDS (2000)	Discoverer designation	Epoch Julian year	Fil.	θ (°)	ρ (″)
14083 + 2112	STF1804	2016.4882	I	14.01 ± 0.14	4.796 ± 0.014
14100 + 0401	STF1805	2016.4882	I	33.60 ± 0.14	4.837 ± 0.014
14134 + 0524	STF1813	2016.4882	I	193.54 ± 0.14	4.703 ± 0.014
14165 + 2007	STF1825	2016.4882	I	153.51 ± 0.14	4.369 ± 0.013
14279 + 2123	HO 543	2016.4882	I	237.37 ± 0.14	4.631 ± 0.014
14506 − 0001	STF1885	2016.4882	I	145.70 ± 0.14	4.100 ± 0.012
15276 + 0522	STF1943	2016.4883	I	148.27 ± 0.14	5.094 ± 0.015
15589 + 2147	STF1990 BC	2016.4883	I	26.34 ± 0.14	4.048 ± 0.012
16003 + 1140	STF1992 AB,C	2016.4883	I	326.35 ± 0.14	5.946 ± 0.018
17178 + 0733	J 450	2016.4896	R	60.99 ± 0.14	4.651 ± 0.014
17268 + 2240	J 1032	2016.4896	R	350.78 ± 0.14	4.057 ± 0.012
17324 + 2352	STF2182 AB	2016.4896	R	0.86 ± 0.14	5.418 ± 0.016
17362 + 0637	STF2188	2016.4896	R	203.71 ± 0.14	5.516 ± 0.016
17590 + 0202	STF2252 AB	2016.4896	R	24.26 ± 0.14	3.948 ± 0.012
18106 + 0349	FOX 220	2016.4896	R	75.37 ± 0.14	5.977 ± 0.018
18148 + 1153	ROE 143	2016.4896	R	90.40 ± 0.14	4.207 ± 0.013
18154 + 1946	STT 346	2016.4896	R	329.58 ± 0.14	5.208 ± 0.015
18206 + 2248	STF2310	2016.4896	R	237.96 ± 0.14	5.052 ± 0.015
18247 − 0636	STF2313	2016.4896	R	196.00 ± 0.14	5.857 ± 0.017
18258 + 0359	J 462	2016.4896	R	348.32 ± 0.14	4.180 ± 0.012
18266 + 0627	GCB 31	2016.4896	R	75.87 ± 0.14	4.501 ± 0.013

TABLE 2

ASTROMETRIC MEASUREMENTS OF THE OBSERVED DOUBLE STARS WITH NO CALCULATED ORBITS

WDS (2000)	Discoverer designation	Epoch 2016+	Fil.	θ (°)	$\delta\theta$ (°)	ρ (″)	$\delta\rho$ (″)
14216 + 1315	HEI 531	0.4919	R	260.5	0.3	1.367	0.011
14222 + 0513	HDS2023	0.4919	R	129.5	0.3	0.455	0.006
14222 + 1350 *	HDS2022	0.4919	R	54.3	0.3	0.338	0.005
14227 + 0216	HDS2025	0.4919	R	14.4	0.2	0.689	0.004
14236 + 2009	COU 184	0.4919	R	113.8	0.2	0.950	0.009
14242 + 0001	RST5385	0.4919	R	357.3	0.6	0.397	0.006
14249 − 0912	RST3876	0.4919	R	23.4	0.4	0.699	0.007
14252 − 0546	RST4527	0.4919	R	108.4	0.6	0.428	0.006
14262 − 0950	RST3878	0.4919	R	67.4	1.5	0.457	0.006
14263 + 0152	HDS2033	0.4919	R	234.4	0.4	0.582	0.007
14276 + 2037	HO 542	0.4919	R	33.2	0.2	1.007	0.009
14286 − 0856	RST3880	0.4919	R	176.4	0.6	0.731	0.008
14286 + 1818	COU2508	0.4919	R	67.3	0.3	0.486	0.006
14293 + 0018	HDS2043 Aa,Ab	0.4919	R	47.3	0.5	0.699	0.007
14293 + 1318	HDS2042	0.4919	R	118.5	0.4	0.310	0.005
14305 + 2055	COU 97	0.4919	R	254.4	0.4	0.276	0.005
14325 + 0308	A 2226 AB	0.4919	R	80.5	0.2	0.461	0.006
14330 + 0656	YSC 6	0.4919	R	105.9	0.2	0.183	0.004
14333 + 2725	A 688	0.4919	R	16.4	0.2	0.764	0.008
14339 + 2949	AGC 6	0.4919	R	134.3	0.2	0.767	0.008
14340 − 0507	A 2589	0.4920	R	203.5	0.2	1.036	0.009
14354 + 1915	HU 574	0.4920	R	112.4	0.2	0.150	0.004
14356 + 1554	HEI 233	0.4920	R	5.2	0.2	1.129	0.010
14359 + 1200	HU 1269	0.4920	R	203.4	0.2	0.368	0.005
14367 + 2014	COU 98	0.4920	R	173.4	0.6	0.187	0.004
14369 − 0417	HDS2061	0.4920	R	148.7	0.2	0.701	0.007
14376 + 2809	COU 405	0.4920	R	105.6	0.7	1.496	0.012
14376 + 3137	HDS2062	0.4920	R	121.4	0.2	0.123	0.004
14394 − 0733	RST3889	0.4920	R	220.3	0.4	0.548	0.007
14401 + 0246	HDS2069	0.4920	R	80.5	0.4	0.481	0.006
14401 + 0504	A 1107	0.4920	R	89.5	0.2	0.333	0.005
14416 + 2747	COU 407	0.4920	R	113.5	0.2	0.428	0.006

TABLE 2. CONTINUED

14417 + 0932	STF1866	0.4920	R	205.2	0.2	0.761	0.008
14419 + 1847	COU 185	0.4920	R	305.9	0.3	0.899	0.009
15261 + 1810	STF1940	0.4974	R	332.4	0.2	0.370	0.005
15262 + 1418	HEI 236	0.4974	R	107.5	0.3	0.523	0.006
15268 + 2840	COU 484	0.4975	R	263.4	0.2	0.333	0.005
16013 − 0658	BU 623	0.4920	R	225.6	0.2	0.733	0.008
16043 − 0313	RST4558	0.4921	R	170.3	0.3	0.580	0.007
16049 + 0213	HEI 793	0.4921	R	196.1	0.2	1.523	0.012
16062 + 1809	COU2389	0.4921	R	238.5	0.2	1.126	0.010
16071 + 1654	BU 812	0.4921	R	97.4	0.2	0.731	0.007
16072 + 1848 *	COU 196	0.4921	R	349.6	1.9	1.584	0.013
16080 + 0559	TDS9770	0.4921	R	256.3	0.3	0.582	0.007
16087 + 0524	HDS2278	0.4921	R	112.4	0.2	0.281	0.005
16092 − 0549	RST4559	0.4921	R	296.4	0.4	0.975	0.009
16092 − 1057 *	HDS2279	0.4921	R	325.5	0.4	0.335	0.005
16097 − 0633	RST3932	0.4921	R	137.4	0.8	0.212	0.005
16139 + 0123	RST5407	0.4921	R	223.3	0.2	0.972	0.009
16152 − 0709	RST3938	0.4921	R	209.5	0.3	1.249	0.011
16168 + 1447	HDS2301	0.4921	R	55.4	0.2	1.007	0.009
16169 + 1948	COU 107	0.4921	R	114.4	0.2	0.637	0.007
16173 + 1626	YSC 153	0.4921	R	131.4	0.3	0.338	0.005
16174 + 0643 *	TDS9822	0.4921	R	349.6	0.4	0.546	0.007
16177 + 1342	YSC 154	0.4921	R	44.9	0.4	0.682	0.007
16186 + 1247	HEI 241	0.4921	R	59.5	0.3	0.763	0.008
16581 + 0902	HDS2401	0.4922	R	17.5	0.2	0.332	0.005
16581 + 1509	STT 319	0.4922	R	65.8	0.1	0.858	0.008
16584 + 1358	YSC 61	0.4922	R	260.4	1.0	0.608	0.007
16594 + 1419	STT 321	0.4922	R	15.3	0.2	0.581	0.007
16595 + 0942	BU 1298 AB	0.4922	R	133.3	0.2	0.429	0.006
17003 + 0106	A 2235	0.4922	R	269.4	0.3	0.827	0.008
17012 + 0627 *	HDS2409	0.4922	R	37.4	0.7	0.274	0.005
17042 + 1834 *	TDT 197	0.4922	R	91.4	0.4	0.396	0.006
17046 − 0339	RST4565	0.4922	R	164.6	0.3	0.823	0.008
17050 + 0724	TDT 204	0.4922	R	152.3	0.3	0.638	0.007
17080 − 0957	RST3966	0.4922	R	111.0	1.2	0.487	0.006
17086 + 0951	HU 167	0.4922	R	272.6	0.5	0.820	0.008
17088 + 0002	A 2237	0.4922	R	69.9	0.3	0.918	0.009
17107 + 1651	HEI 167	0.4922	R	98.4	0.3	0.394	0.006
17107 + 2104 *	TDT 251	0.4922	R	122.4	0.4	0.544	0.007
17107 + 2312 *	TDT 250	0.4922	R	11.0	0.3	0.795	0.008
17110 + 0302	HDS2426	0.4922	R	195.4	0.3	0.883	0.009
17110 + 1622	HEI 168	0.4922	R	65.7	0.2	0.763	0.008
17136 + 0405	HEI 895	0.4922	R	15.5	1.7	0.854	0.009
17140 + 2119	COU 111	0.4923	R	249.5	0.3	0.613	0.007
17142 + 2731	COU 495	0.4923	R	100.6	0.4	0.819	0.008
17150 + 1238 *	HDS2439	0.4923	R	168.9	0.5	0.518	0.006
17155 + 2007	HU 489	0.4923	R	35.8	0.2	1.035	0.009
17160 + 1702 *	TDT 294	0.4923	R	77.6	0.5	0.582	0.007
17174 + 1939	COU 496 AB	0.4923	R	172.0	0.9	0.823	0.008
17182 + 1559	HEI 246	0.4923	R	45.3	0.3	1.160	0.010
17247 + 3802	COU1142 AB	0.4977	R	222.4	0.2	1.858	0.014
17272 + 3235 *	TDT 362	0.4977	R	156.4	0.4	0.310	0.005
17285 + 3657	COU1143	0.4977	R	244.4	0.3	0.370	0.005
17290 + 3845	COU1297	0.4977	R	99.4	0.3	0.276	0.005
17293 + 3758	HO 417	0.4977	R	306.4	0.2	0.310	0.005
17345 + 3935	COU1298	0.4977	R	251.5	0.2	0.302	0.005
17354 + 3443	COU 995	0.4977	R	335.3	0.2	0.421	0.006
17359 + 3205	COU 807	0.4977	R	143.4	0.3	0.670	0.007
17455 + 3554	HDS2509	0.4977	R	74.9	0.2	0.548	0.006
17462 + 3853	COU1300	0.4977	R	125.7	0.2	0.765	0.008
17464 + 3553 *	TDT 497	0.4977	R	263.8	0.3	0.761	0.008
17470 + 3750	COU1144	0.4977	R	283.9	0.2	0.941	0.009
17471 + 3235	COU 634	0.4977	R	79.4	0.3	0.246	0.005
17504 + 3526	ORL 1 Aa,Ab	0.4977	R	29.4	0.2	0.304	0.005
17512 + 3821	HU 1183	0.4977	R	191.4	0.2	0.489	0.006

TABLE 2. (CONTINUED)

17528 + 3408 *	TDT 553	0.4977	R	62.4	0.3	0.702	0.007
17553 + 3532	A 2987 AC	0.4977	R	60.9	0.2	1.402	0.012
17569 + 3236	HU 1184	0.4977	R	204.6	0.2	0.916	0.009
17583 + 3329	HO 74 AB	0.4977	R	124.8	0.2	3.287	0.023
17583 + 3329	COU1001 Aa,Ab	0.4977	R	220.5	0.2	0.483	0.006
17584 + 2233 *	TDS 893	0.4923	R	279.8	0.5	0.766	0.008
17584 + 3524	COU1000	0.4977	R	154.4	0.2	0.944	0.009
17587 + 3538	COU1002	0.4977	R	163.7	0.2	0.853	0.008
17592 + 3926	COU1458	0.4977	R	78.4	0.4	0.364	0.005
18000 + 2449	COU 115	0.4950	R	118.5	0.2	0.278	0.005
18007 + 1736	COU 810	0.4950	R	99.4	0.4	0.157	0.004
18009 + 2432 *	TDT 636	0.4950	R	185.4	0.7	0.167	0.004
18036 + 3731	COU1147	0.4950	R	178.2	0.2	0.737	0.008
18036 + 3731	COU1147	0.4978	R	178.2	0.2	0.737	0.008
18047 + 4650 *	COU2115	0.4950	R	41.9	0.8	0.274	0.005
18048 + 5344 *	HDS2546	0.4950	R	235.5	0.4	0.578	0.007
18054 + 4306	COU1787	0.4951	R	325.4	0.3	0.395	0.006
18054 + 5155	COU2513	0.4951	R	57.6	0.2	0.915	0.009
18058 + 3512	TDT 678	0.4978	R	236.4	0.4	0.669	0.007
18062 + 3326	HO 79	0.4978	R	61.4	0.9	0.216	0.005
18070 + 3323 *	TDT 689	0.4978	R	242.4	1.0	0.366	0.006
18104 + 5104	COU2392	0.4951	R	147.3	0.3	0.641	0.007
18109 + 3321	COU1005 AB,C	0.4978	R	25.4	0.4	1.889	0.015
18109 + 3321	COU1005 AB	0.4978	R	333.4	0.4	0.211	0.005
18110 + 5038	HDS2564	0.4951	R	306.4	0.3	0.364	0.005
18112 + 3906	HDS2565	0.4978	R	340.1	0.2	0.670	0.007
18114 + 2519	A 238	0.4924	R	71.6	0.2	0.636	0.007
18118 + 3327	HO 82 AB,C	0.4978	R	220.7	0.2	0.701	0.007
18119 + 4733	COU2117	0.4951	R	298.5	0.3	0.426	0.006
18121 + 2739	STF2292	0.4924	R	276.9	0.2	0.885	0.008
18127 + 5446	MLR 585	0.4951	R	335.4	0.3	0.428	0.006
18132 + 5749 *	HDS2571	0.4951	R	310.4	0.4	0.274	0.005
18133 + 0906	HDS2573	0.4924	R	165.4	0.2	0.853	0.008
18133 + 2118	TDT 743	0.4924	R	67.8	1.0	1.004	0.010
18133 + 5242	A 1376	0.4951	R	203.4	0.3	0.338	0.005
18134 + 1643	HEI 170	0.4924	R	313.4	0.4	0.337	0.005
18139 + 3212 *	TDT 749	0.4978	R	15.4	0.7	0.167	0.004
18144 + 1953	HDS2576	0.4924	R	68.1	0.3	0.966	0.009
18145 + 3249	HU 927	0.4978	R	102.4	0.2	0.369	0.005
18145 + 3313	COU1007	0.4978	R	38.4	0.3	0.274	0.005
18177 + 3932 *	TDT 778	0.4978	R	177.4	0.5	0.914	0.009
18182 + 5337	MLR 586	0.4951	R	194.4	0.2	0.636	0.007
18208 + 3639	COU1306	0.4978	R	42.4	0.3	0.454	0.006
18212 + 3917	COU1460	0.4978	R	341.5	0.2	0.452	0.006
18217 + 5740	MLR 536	0.4951	R	194.7	0.3	0.851	0.008
18222 + 3417 *	TDT 818	0.4978	R	205.4	0.4	0.273	0.005
18238 + 5318 *	YSC 66	0.4951	R	42.7	0.2	0.914	0.009
18243 + 3609	HDS2603	0.4978	R	353.7	0.3	0.853	0.008
18250 − 0517	RST4587	0.4895	R	332.3	0.3	0.395	0.006
18252 + 5659	MLR 537	0.4951	R	56.5	0.2	0.579	0.007
18253 + 2805	HDS2604 Aa,Ab	0.4924	R	212.1	0.3	0.729	0.008
18256 + 3945	COU1461	0.4978	R	245.1	0.3	0.790	0.008
18266 + 0633	HDS2607	0.4896	R	243.4	0.5	0.151	0.004
18272 + 0012	STF2316 AB	0.4896	R	321.7	0.2	3.749	0.026
18279 + 0124	HDS2614	0.4896	R	333.3	0.3	0.704	0.007
18283 + 0537 *	TDT 897	0.4896	R	169.4	0.4	0.489	0.006
18285 + 2010	COU 203	0.4896	R	60.5	0.3	0.488	0.006
18285 + 2010	COU 203	0.4924	R	60.5	1.1	0.486	0.006
18289 + 1815	COU 507	0.4896	R	154.0	0.4	0.947	0.009
18291 + 0408	A 581 AB	0.4896	R	139.5	0.3	0.392	0.006
18297 + 3929	TDT 910	0.4978	R	195.6	0.2	0.821	0.008
18298 + 5314	TDT 911	0.4951	R	196.4	0.3	0.734	0.008
18301 + 5805	MLR 357	0.4951	R	204.3	0.4	0.582	0.007
18303 + 1907	COU 508	0.4896	R	253.7	0.3	0.910	0.009
18304 + 1348	HU 583	0.4896	R	307.3	0.2	0.759	0.008

TABLE 2. (CONTINUED)

18305 + 0416	A 583	0.4896	R	265.4	0.4	0.177	0.004
18309 + 3417	COU1150 Aa,Ab	0.4978	R	265.4	0.2	0.214	0.004
18310 + 0712 *	TDT 924	0.4897	R	318.3	0.6	0.611	0.007
18310 + 2424	TDT 923	0.4897	R	328.6	0.2	0.823	0.008
18312 + 2516	A 248	0.4897	R	34.5	0.3	0.490	0.006
18314 + 0802	HDS2627	0.4897	R	211.4	0.2	0.457	0.006
18316 + 2030	COU 119	0.4897	R	229.2	0.3	0.673	0.007
18319 + 3538	COU1151	0.4978	R	280.0	0.2	1.310	0.011
18321 + 1359	J 1133	0.4897	R	125.4	1.9	2.254	0.017
18324 + 3231 *	TDT 932	0.4978	R	320.3	0.2	0.512	0.006
18325 + 0036	RST5450	0.4897	R	254.4	0.4	0.703	0.007
18327 + 1741	TDT 934	0.4897	R	128.2	0.3	0.820	0.008
18332 + 3420 *	TDT 935	0.4978	R	174.9	0.5	0.868	0.009
18335 + 3510	HO 86	0.4978	R	199.5	0.2	0.307	0.005
18385 + 3503	COU1308	0.4978	R	28.5	0.2	0.422	0.006
18402 + 3822	HDS2644	0.4978	R	76.4	0.2	0.095	0.004
18402 + 5048	COU2515	0.4951	V	276.4	0.7	0.334	0.005
18405 + 3139	HO 437 AB	0.4978	R	140.4	0.2	0.270	0.005
18423 + 3616	A 1381	0.4978	R	94.4	0.2	0.367	0.005
18432 + 3822	HDS2651	0.4978	R	52.2	0.3	0.481	0.006
18448 + 5201	HU 755	0.4951	V	125.4	0.3	0.579	0.007
18453 + 3856	COU1608	0.4979	R	230.0	0.3	1.070	0.010
18459 + 3657	COU1309	0.4979	R	180.4	0.4	0.482	0.006
18461 + 5212	MLR 637	0.4951	V	102.1	0.5	0.763	0.008
18465 + 3414	COU1153	0.4979	R	115.5	0.3	0.393	0.006
18466 + 5142	HU 756	0.4952	V	262.8	0.3	1.036	0.009
18476 + 3248	COU1154	0.4979	R	56.5	0.3	0.578	0.007
18481 + 3929	COU1609	0.4979	R	201.7	0.4	0.822	0.008
18490 + 3432	YSC 11	0.4979	R	54.9	0.2	0.359	0.005
18490 + 3914	COU1610	0.4979	R	144.5	0.4	0.399	0.006
18499 + 5516	MLR 574	0.4952	V	54.7	0.3	1.093	0.010
18521 + 2431	COU 510	0.4924	R	181.4	0.9	0.185	0.005
18525 + 2632	HDS2677 Aa,Ab	0.4924	R	80.2	0.5	1.030	0.010
18527 + 5842	HDS2678	0.4952	V	33.7	0.9	0.659	0.007
18528 + 3125	A 257 CD	0.4924	R	262.8	0.9	0.759	0.008
18528 + 3125	A 257 CD	0.4979	R	262.7	0.3	0.758	0.008
18528 + 3125	A 257 AB	0.4924	R	95.1	0.3	0.914	0.009
18552 + 3941	TDT1126	0.4979	R	190.5	0.5	0.362	0.005
18554 + 3556	A 1385 AB	0.4979	R	295.4	0.3	0.454	0.006
18555 + 3215	COU1013	0.4979	R	147.4	0.3	0.643	0.007
18557 + 5714	TDT1129	0.4952	V	14.3	1.7	0.549	0.007
18563 + 5432 *	HDS2682 Aa,Ab	0.4952	V	327.4	0.6	0.366	0.006
18563 + 5432 *	HDS2682 Aa,Ab	0.4952	V	326.5	0.6	0.366	0.006
18564 + 5854	TDS 955	0.4952	V	149.3	0.4	0.914	0.009
18571 + 3451	HDS2685	0.4979	R	200.3	0.2	0.515	0.006
18572 + 3845	COU1611	0.4979	R	111.5	0.4	0.643	0.007
18576 + 3209	A 260	0.4979	R	246.3	0.2	0.911	0.009
18586 + 5210	MLR 638	0.4952	V	131.5	0.3	0.278	0.005
18589 + 3229	BU 649	0.4979	R	1.0	0.2	1.832	0.014
18593 + 5450	A 1387 AB	0.4952	V	351.4	0.3	0.331	0.005
19006 + 3300	COU1156	0.4979	R	110.8	0.2	0.793	0.008
19006 + 3951	COU1933	0.4979	R	197.3	0.2	0.552	0.006
19006 + 3952	HDS2696	0.4979	R	138.4	0.2	0.302	0.005
19016 + 3253	HU 1295	0.4979	R	223.4	0.4	0.272	0.005
19018 + 3448	COU1612	0.4979	R	322.4	0.3	0.883	0.009
19020 + 3210	HU 1296	0.4979	R	195.4	0.8	0.119	0.004
19023 + 3328	COU1312	0.4979	R	235.4	0.4	0.270	0.005
19024 + 3608	COU1613	0.4979	R	318.5	0.4	0.545	0.007
19028 + 2208 *	TDS 961	0.4925	R	215.0	0.3	0.885	0.009
19034 + 2511	A 2991	0.4925	R	84.1	0.3	0.734	0.008
19036 + 3705	HDS2702	0.4979	R	266.4	0.5	0.168	0.004
19050 + 5553	A 1389	0.4952	R	231.4	0.3	0.249	0.005
19056 + 2724	HDS2709	0.4925	R	43.4	0.4	0.331	0.005
19057 + 2717	HO 95	0.4925	R	143.4	0.3	0.208	0.004
19061 + 3549	COU1614	0.4979	R	121.4	0.2	0.577	0.007
19064 + 3144	HO 97 AB	0.4925	R	196.6	0.2	0.762	0.008

TABLE 2. (CONTINUED)

19066 + 2646	COU 722	0.4925	R	336.3	0.2	1.063	0.010
19074 + 3601	COU1615	0.4979	R	96.4	0.4	0.426	0.006
19081 + 3031	HO 99	0.4925	R	167.4	0.3	0.396	0.006
19082 + 3829	COU1936 AB	0.4979	R	124.3	0.4	0.550	0.007
19086 + 5208	MLR 639	0.4952	R	37.4	0.3	0.392	0.006
19086 + 5531 *	TDS 967	0.4952	R	153.3	0.3	0.973	0.009
19087 + 5630	MLR 577	0.4952	R	277.2	0.3	0.762	0.008
19103 + 3044	COU1020	0.4925	R	100.7	0.3	1.035	0.009
19150 + 5528	TDT1319	0.4952	R	65.6	0.3	0.855	0.008
19158 + 5458	A 1392	0.4952	R	277.4	0.2	0.151	0.004
19165 + 5003	COU2627	0.4952	R	22.4	0.6	0.186	0.004
19178 + 5950	HDS2729	0.4952	R	161.4	0.3	0.093	0.004
19186 + 5358	A 1393	0.4952	R	256.4	0.2	0.704	0.007
19195 + 5729	MLR 539	0.4952	R	192.4	0.3	0.248	0.005
19207 + 5811 *	TDT1387	0.4952	R	300.3	0.3	0.819	0.008
19213 + 5817	TDT1395	0.4952	R	168.7	0.2	0.857	0.008
19221 + 5347 *	TDT1403	0.4952	R	125.4	0.3	0.515	0.006
19228 + 5637	A 708	0.4952	R	170.6	0.2	1.007	0.009
19251 + 2213	COU 513	0.4925	R	6.4	0.3	0.271	0.005
19266 + 2619	HDS2763	0.4925	R	208.9	0.3	0.792	0.008
19290 + 1515	A 1651	0.4897	R	253.4	0.3	0.184	0.004
19301 − 0735	RST4630	0.4897	R	290.4	1.0	0.362	0.006
19303 + 0333	TDT1506	0.4897	R	16.8	0.5	0.729	0.008
19305 + 1151	HEI 573	0.4897	R	226.7	0.4	0.885	0.009
19307 + 1439 *	TDT1512	0.4897	R	324.5	0.5	0.552	0.007
19310 + 0429	A 366	0.4897	R	304.4	0.3	0.489	0.006
19311 + 0824	A 1184	0.4897	R	114.2	0.2	0.879	0.008
19311 + 0829 *	TDT1516	0.4897	R	358.1	0.4	0.822	0.008
19321 + 0858 *	TDT1527	0.4898	R	159.4	0.6	0.457	0.006
19321 + 1206	TDT1526	0.4898	R	132.3	0.4	0.548	0.007
19326 + 0435 *	TDS 999	0.4898	R	343.8	0.4	0.972	0.009
19326 + 1203	HEI 574	0.4898	R	150.5	0.2	0.455	0.006
19334 − 0602	RST4632	0.4898	R	53.7	0.9	0.731	0.008
19342 + 0747 *	HDS2777	0.4898	R	252.4	0.2	0.186	0.004
19343 + 0021	HDS2779	0.4898	R	214.4	0.3	0.273	0.005
19383 + 5535	TDT1597	0.4953	R	125.4	0.3	0.667	0.007
19395 + 5748 *	TDT1608	0.4953	R	121.4	0.3	1.097	0.010
19400 + 5545	A 1403	0.4953	R	166.4	0.4	0.209	0.004
19411 + 5811	A 716	0.4953	R	284.5	0.3	0.454	0.006
20087 + 5320	A 1417	0.4953	R	173.4	0.2	0.621	0.007
20096 + 5034	TDT2035	0.4953	R	91.7	0.3	0.788	0.008
20176 + 5113 *	TDS1056	0.4953	R	256.2	0.3	1.436	0.012
20183 + 5152	HDS2900	0.4953	R	286.4	0.2	0.149	0.004
20185 + 5542	BU 1260	0.4953	R	135.4	0.3	0.340	0.005
20187 + 5823	TDT2157	0.4953	R	37.3	0.3	0.788	0.008
20196 + 5132	TDT2169	0.4953	R	52.9	0.2	0.914	0.009
20232 + 5946	MLR 432	0.4953	R	216.4	0.3	0.184	0.004
20239 + 5232	A 1428	0.4953	R	205.4	0.2	0.333	0.005
20239 + 5420	HDS2914	0.4953	R	213.4	0.6	0.211	0.005
20246 + 5527	MLR 588	0.4953	R	245.4	0.2	0.242	0.005
20257 + 5508	A 1429	0.4953	R	187.4	0.2	0.641	0.007
20278 + 5456	TDT2293	0.4953	R	81.4	0.3	0.762	0.008
20298 + 5654 *	TDT2322	0.4953	R	19.5	1.6	1.676	0.014
20310 + 5953	HDS2933	0.4953	R	8.6	0.3	0.427	0.006
20312 + 5714	A 872	0.4953	R	178.4	0.4	0.214	0.005
20315 + 5520	TDS1079	0.4953	R	125.5	0.2	0.880	0.008
20316 + 0530	A 395	0.4898	R	161.6	0.5	0.642	0.007
20318 + 5128	TDT2339	0.4953	R	338.4	0.3	0.976	0.009
20329 + 1357	BU 670 AB	0.4898	R	6.4	0.2	0.851	0.008
20329 + 1906	COU2644	0.4898	R	290.4	0.3	0.822	0.008
20331 + 2324	A 2792	0.4898	R	305.4	0.6	0.214	0.005
20334 − 0321	HDS2936	0.4898	R	156.4	0.5	0.244	0.005
20335 + 0527	STF2696 AB	0.4899	R	299.4	0.2	0.520	0.006
20339 + 1106 *	TDT2376	0.4899	R	76.1	0.4	0.761	0.008
20342 + 1333	HEI 277	0.4899	R	247.4	0.3	0.697	0.007
20348 + 1726	COU 223	0.4899	R	161.4	0.5	0.393	0.006

TABLE 2. (CONTINUED)

20349 + 1120	TDT2394	0.4899	R	1.5	0.2	0.455	0.006
20351 − 0436	RST4671	0.4899	R	227.5	0.2	0.730	0.008
20354 + 1121	YR 16	0.4899	R	278.4	0.4	0.701	0.008
20381 + 2953	A 744	0.4925	R	274.3	0.2	0.732	0.008
20383 + 2106 *	TDT2441	0.4925	R	269.2	0.3	0.608	0.007
20384 + 2455	TDT2446	0.4925	R	99.5	0.4	0.459	0.006
20385 + 2945	COU1172	0.4925	R	279.5	0.4	0.336	0.005
20386 + 2007	COU 225	0.4925	R	286.4	0.8	0.277	0.005
20390 + 3702	COU2219	0.4981	R	45.2	0.3	0.941	0.009
20393 + 2714	TDT2454 Ba,Bb	0.4926	R	46.3	0.3	0.916	0.009
20397 + 3658	A 1432	0.4981	R	117.4	0.3	0.432	0.006
20401 + 3044	TDT2457 Aa,Ab	0.4926	R	138.5	0.4	0.888	0.009
20406 + 2156	A 2795	0.4926	R	240.4	0.2	0.246	0.005
20410 + 3218	STF2716 AB	0.4981	R	46.4	0.1	2.772	0.020
20411 + 2751 *	TDT2471	0.4926	R	2.4	0.8	0.240	0.005
20411 + 3516	COU1963 AB,C	0.4981	R	48.4	0.2	1.645	0.013
20411 + 3516	COU1963 AB	0.4981	R	180.4	0.2	0.213	0.004
20412 + 2023	COU 423	0.4926	R	162.4	0.4	0.401	0.006
20416 + 3000	COU1174	0.4926	R	32.4	0.4	0.339	0.005
20416 + 3950	COU2290	0.4981	R	43.3	0.2	0.545	0.006
20424 + 3455	COU1965	0.4981	R	277.5	0.2	0.365	0.005
20432 + 3350	HDS2949	0.4981	R	166.4	0.2	0.944	0.009
20433 + 2616	COU1039	0.4926	R	237.1	0.4	1.035	0.009
20440 + 3839	COU2292	0.4981	R	240.4	0.2	0.309	0.005
20445 + 3409	HU 690	0.4981	R	281.5	0.2	0.490	0.006
20447 + 2703 *	TDT2515	0.4926	R	277.5	0.6	0.400	0.006
20451 + 3529	COU1809	0.4981	R	101.4	0.3	0.731	0.008
20459 + 3852 *	COU2294	0.4982	R	124.9	0.3	0.857	0.008
20460 + 3554 *	TDT2525	0.4982	R	70.3	0.3	0.579	0.007
20463 + 2853 *	TDT2530	0.4926	R	207.3	0.3	0.606	0.007
20464 + 3511	COU1810	0.4982	R	183.4	0.5	0.187	0.004
20475 + 3016	COU1176	0.4926	R	225.4	0.4	0.366	0.005
20477 + 3258	COU1634	0.4982	R	61.4	0.4	0.395	0.006
20480 + 3917	A 1434 AB,C	0.4982	R	255.9	0.2	2.513	0.018
20482 + 2622	COU 827 Aa,Ab	0.4926	R	329.4	0.3	0.574	0.007
20487 + 2943 *	TDT2556	0.4926	R	280.4	0.2	0.790	0.008
20490 + 2540 *	HDS2966	0.4926	R	229.4	0.2	0.518	0.006
20490 + 2637	COU 828 AB	0.4927	R	188.5	0.2	0.913	0.009
20490 + 3619	COU1811	0.4982	R	255.4	0.3	0.759	0.008
20503 + 5937	MLR 239	0.4954	R	286.3	0.3	0.888	0.009
20531 + 2909	STT 417 AB	0.4927	R	28.5	0.2	0.917	0.009
20535 + 2630	COU1177	0.4927	R	14.4	0.4	0.248	0.005
20547 + 2516	COU 830	0.4927	R	168.8	0.3	1.039	0.009
20573 + 2345 *	TDT2656	0.4927	R	349.4	0.2	0.735	0.008
21009 + 5929	MLR 241	0.4954	R	174.6	0.2	0.948	0.009
21012 + 5953 *	TDT2696	0.4954	R	67.3	0.3	0.519	0.006
21035 + 5925	MLR 243	0.4954	R	224.4	0.6	0.211	0.005
21036 + 5358	HDS2999 Aa,Ab	0.4954	R	351.5	0.2	0.337	0.005
21055 + 5340	BU 680 AB	0.4954	R	284.5	0.2	0.635	0.007
21067 + 5556	TDT2753	0.4954	R	211.4	0.3	0.704	0.007
21096 + 0550 *	TDT2793	0.4899	R	173.4	0.5	0.336	0.005
21106 + 1650	HU 367	0.4899	R	339.4	0.2	0.331	0.005
21118 + 5959	STF2780 AB	0.4954	R	214.1	0.1	1.037	0.009
21119 + 2758 *	TDT2814	0.4927	R	290.4	0.4	2.254	0.017
21142 + 1231	HEI 406	0.4899	R	180.2	0.3	0.704	0.007
21152 + 2753	COU 531	0.4927	R	144.2	0.2	0.943	0.009
21152 + 5531	A 1692	0.4954	R	167.4	0.2	0.272	0.005
21160 + 5914 *	TDT2869	0.4954	R	113.3	0.5	0.674	0.007
21196 + 5552	MLR 582	0.4954	R	347.5	0.3	0.948	0.009
21197 + 5455	A 1694	0.4954	R	94.6	0.2	0.850	0.008
21199 + 5319	A 1695	0.4954	R	193.5	0.2	0.483	0.006
21200 + 5436	TDT2908 Aa,Ab	0.4954	R	115.4	0.5	0.306	0.005
21202 + 5411	HDS3036	0.4954	R	165.4	0.2	0.392	0.005
21203 + 5354	TDT2910	0.4954	R	286.6	0.2	0.675	0.007
21227 + 5214	HU 591	0.4954	R	129.5	0.2	0.761	0.008

TABLE 2. (CONTINUED)

21237 + 5518	A 1892	0.4954	R	350.1	0.2	0.766	0.008
21249 + 5734	A 766	0.4954	R	228.3	0.3	0.486	0.006
21251 + 5229	HU 592	0.4954	R	325.4	0.2	0.823	0.008
21252 + 5618	TDS1127	0.4954	R	235.7	0.2	1.097	0.010
21263 + 5951	MLR 361	0.4954	R	268.4	0.3	0.606	0.007
21273 + 5953	MLR 362	0.4954	R	55.5	0.3	0.338	0.005
21274 + 5835	MLR 435	0.4954	R	236.4	0.5	0.181	0.004
21287 + 5710	BU 1142	0.4954	R	5.5	0.4	0.369	0.005
21327 + 5459 *	HDS3063	0.4954	R	2.4	0.2	0.339	0.005
21346 + 5633	A 1893 AB	0.4954	R	28.3	0.2	0.641	0.007
21362 + 5139	HDS3075	0.4954	R	15.9	0.2	0.609	0.007
21372 + 5346	MLR 609	0.4954	R	40.5	0.2	1.035	0.009
21376 + 5546	BU 686 AB	0.4954	R	311.2	0.2	1.004	0.009
21377 + 5659	MLR 583	0.4954	R	15.2	0.3	0.789	0.008
21377 + 5734	D 25 AB	0.4955	R	163.6	0.2	0.974	0.009
21378 + 5333 *	TDT3067	0.4955	R	33.6	0.2	0.821	0.008
21398 + 5403	TDT3093	0.4955	R	332.5	0.4	0.398	0.006
21399 + 5533	TDT3096	0.4955	R	36.3	0.4	1.032	0.009
22016 + 5654 *	TDT3295	0.4955	R	42.4	1.1	0.179	0.005
22033 + 5403 *	TDT3313	0.4955	R	133.3	0.4	0.886	0.009
22045 + 5239	HU 776	0.4955	R	357.4	0.8	0.164	0.004
22056 + 5711	BAR 57 AB	0.4955	R	274.5	0.4	0.976	0.009
22075 + 5631	HDS3141	0.4955	R	330.5	0.2	0.514	0.006
22077 + 5020	COU2550	0.4955	R	114.2	0.2	0.673	0.007
22078 + 5333	MLR 592	0.4955	R	22.4	0.3	0.488	0.006
22080 + 5635	HDS3144	0.4955	R	33.4	0.2	0.166	0.004
22093 + 5804	MLR 557	0.4955	R	304.6	0.3	0.970	0.009
22107 + 5830	A 624	0.4955	R	14.4	0.2	0.763	0.008
22115 + 5110	COU2660	0.4955	R	250.2	0.3	0.670	0.007
22115 + 5232	COU2659	0.4955	R	161.9	0.3	1.253	0.011
22117 + 5743	A 625 AB	0.4955	R	81.5	0.2	0.551	0.006
22122 + 5909	MLR 439	0.4955	R	253.6	0.2	0.791	0.008

TABLE 3

ASTROMETRIC MEASUREMENTS AND RESIDUALS FOR OBSERVED BINARY STARS WITH CALCULATED ORBITS

WDS (2000)	Discoverer designation	Epoch 2016+	Fil.	θ (°)	$\delta\theta$ (°)	ρ ($''$)	$\delta\rho$ ($''$)	$\theta_O - \theta_C$ (°)	$\rho_O - \rho_C$ ($''$)	Orbit Ref.
14190 − 0636	HDS2016 AB	0.4919	R	325.9	0.3	0.198	0.004	1.5	0.011	Tok2015c
14231 + 0729	A 1104	0.4919	R	244.4	0.2	0.423	0.006	1.3	-0.058	Izm2019
14267 + 1625	A 2069	0.4919	R	102.4	0.3	0.159	0.004	24.8	0.034	Sca2001g
14426 + 1929	HU 575 AB	0.4920	R	115.4	0.2	0.368	0.005	0.5	0.003	Sod1999
16038 + 1406	HDS2265	0.4921	R	9.4	0.3	0.276	0.005	0.1	0.000	Tok2018e
16059 + 1041	HDS2273 Aa,Ab	0.4921	R	253.5	0.2	0.364	0.005	0.4	0.009	Tok2019h
16079 + 1425	A 1798	0.4921	R	344.4	0.2	0.211	0.004	11.2	0.064	USN2002
16115 + 1507	A 1799	0.4921	R	296.6	0.2	0.817	0.008	1.4	0.024	Zir2014a
16169 + 0113	A 2181	0.4921	R	86.5	0.3	0.518	0.006	-18.8	0.101	Pop1995d
17066 + 0039	TOK 52 Ba,Bb	0.4922	R	18.4	0.2	0.091	0.004	-4.8	-0.008	Izm2019
17066 + 0039	BU 823 AB	0.4922	R	172.0	0.2	1.037	0.009	0.7	-0.004	Izm2019
17136 + 1716	A 2087	0.4923	R	133.4	0.3	0.488	0.006	-1.8	0.016	Mnt2001a
17155 + 1052	HDS2440	0.4923	R	113.4	0.5	0.160	0.004	-7.5	0.021	Cve2014
17176 + 1025	HDS2445	0.4923	R	261.4	0.3	0.215	0.004	1.5	-0.002	Tok2017b
17240 + 3835	HU 1179	0.4977	R	272.4	0.1	0.303	0.005	3.1	0.039	Hrt2000b
17247 + 3802	HSL 1 Aa,Ac	0.4977	R	61.7	0.2	0.254	0.005	3.9	-0.045	Rbr2018
17251 + 3444	HU 922 Aa,Ab	0.4977	R	30.4	0.3	0.275	0.005	0.4	-0.009	FMR2016b
17487 + 3536	HU 1182	0.4977	R	298.5	0.2	0.426	0.006	-0.8	0.021	USN2002
17490 + 3704	COU1145	0.4977	R	103.4	0.2	0.164	0.004	1.0	0.017	Hrt1996a
17591 + 3228	HU 1185	0.4977	R	145.5	0.2	0.394	0.006	1.2	-0.005	Doc2012i
18003 + 2154	A 1374 AB	0.4950	R	215.4	0.2	0.485	0.006	2.2	-0.012	Msn2017a
18017 + 4011	STF2267	0.4950	R	277.5	0.2	0.521	0.006	1.9	0.000	Zir2014a
18025 + 4414	BU 1127 AB	0.4950	R	46.3	0.2	0.701	0.007	0.7	0.000	Cve2016c
18033 + 3921	STF2275	0.4977	R	303.5	0.2	0.336	0.005	-1.5	0.023	Pop2000a

TABLE 3. (CONTINUED)

18033 + 3921	STF2275	0.4950	R	303.5	0.2	0.335	0.005	-1.4	0.022	Pop2000a
18035 + 4032	COU1785	0.4950	R	30.4	0.2	0.166	0.004	-5.0	0.000	Doc2008a
18043 + 4206	COU1786 Aa,Ab	0.4950	R	11.4	0.2	0.152	0.004	12.0	-0.030	Hrt2009
18063 + 3824	HU 1186	0.4978	R	134.4	0.2	0.176	0.004	-29.7	0.104	USN2006b
18092 + 3129	COU 812	0.4923	R	265.6	0.3	0.672	0.007	-21.0	-0.006	Cou1999b
18097 + 5024	HU 674	0.4951	R	214.4	0.2	0.765	0.008	0.6	0.024	Msn2017e
18126 + 3836	BU 1091	0.4978	R	320.3	0.2	0.765	0.008	1.5	0.004	Zir2012b
18130 + 3318	COU1006	0.4978	R	337.4	0.2	0.514	0.006	81.6	0.220	Cou1999b
18154 + 5720	HDS2577	0.4951	R	330.4	0.2	0.186	0.004	10.9	-0.038	RAO2015
18163 + 3625	HU 1291	0.4978	R	52.4	0.2	0.304	0.005	3.0	0.017	Hrt2014b
18250 − 0135	AC 11	0.4895	R	355.7	0.1	0.914	0.009	0.8	0.005	Tok2017c
18261 + 0047	BU 1203	0.4896	R	158.3	0.2	0.518	0.006	0.4	0.021	Pop1996b
18320 + 0647	STT 354	0.4897	R	217.3	0.2	0.549	0.006	2.5	-0.026	Zir2013a
18339 + 5221	A 1377 AB	0.4951	V	134.4	0.1	0.244	0.005	-6.3	0.109	Mut2010e
18421 + 3445	B 2546 Aa,Ab	0.4978	R	24.4	0.2	0.124	0.004	-2.5	0.018	USN2002
18437 + 3141	A 253	0.4979	R	134.2	0.2	0.702	0.007	-2.2	0.094	Baz1987d
18466 + 3821	HU 1191	0.4979	R	338.4	0.2	0.218	0.004	-2.2	-0.009	Doc2009g
18534 + 2553	A 2989	0.4925	R	199.4	0.4	0.309	0.005	-2.0	0.022	USN2002
19039 + 2642	A 2992	0.4925	R	224.4	0.4	0.167	0.004	-3.7	-0.018	Doc2009g
19055 + 3352	HU 940	0.4979	R	191.4	0.2	0.458	0.006	2.0	-0.004	Doc2009g
19073 + 2432	A 262	0.4925	R	269.4	0.3	0.167	0.004	-3.2	-0.034	Zir2012b
19083 + 2706	HO 98 AB	0.4925	R	61.4	0.2	0.209	0.004	5.3	0.030	Lin2012a
19083 + 5520	D 19 AB	0.4952	R	344.5	0.2	0.458	0.006	1.6	-0.034	Hrt2013c
19106 + 5429	A 1391	0.4952	R	22.4	0.3	0.246	0.005	-2.7	0.013	Pru2014
19216 + 5223	BU 1129	0.4952	R	343.4	0.2	0.304	0.005	2.9	-0.014	Baz1984a
19296 + 1224	A 1653	0.4897	R	142.4	0.2	0.210	0.004	7.1	0.013	Pru2014
19330 + 0546	A 367	0.4898	R	306.3	0.2	1.037	0.009	2.2	0.078	Izm2019
19351 + 5038	HU 679	0.4953	R	272.5	0.2	0.397	0.005	3.3	0.001	Ana2005
20306 + 1349	HDS2932	0.4898	R	309.4	0.4	0.122	0.004	-10.1	-0.017	Hor2011b
20311 + 1548	A 1675	0.4898	R	304.4	0.2	0.165	0.004	0.8	0.004	Hrt2001b
20312 + 1116	CHR 99 Aa,Ab	0.4898	R	185.3	0.2	0.307	0.005	-2.8	-0.030	Hrt2014b
20329 + 1357	L 35 CD	0.4898	R	143.5	0.3	0.515	0.006	-0.1	0.032	Hrt2014b
20410 + 3905	MCA 62 Aa,Ab	0.4981	R	276.4	0.2	0.122	0.004	-1.6	0.034	Ole2003c
20444 + 1945	CAR 2	0.4926	R	320.4	0.8	0.218	0.005	13.1	0.008	Cve2017b
20471 + 2525	BU 364	0.4926	R	75.3	0.2	0.731	0.007	2.0	0.005	Izm2019
20474 + 3629	STT 413 AB	0.4982	R	2.6	0.1	0.942	0.009	0.8	0.042	Izm2019
21109 + 2925	BAG 29	0.4927	R	174.4	0.7	0.188	0.004	1.2	0.000	Bag2010
21125 + 2821	HO 152	0.4927	R	158.4	0.3	0.167	0.004	6.2	0.026	Doc2016g
21135 + 0713	BU 270 AB	0.4899	R	345.4	0.2	0.490	0.006	0.7	0.008	Msn2017a
21147 − 0050	A 883 AB	0.4899	R	287.4	0.3	0.160	0.004	0.5	0.013	Hrt2009
22086 + 5917	STF2872 BC	0.4955	R	298.2	0.2	0.848	0.008	1.3	0.046	USN2002

TABLE 4

NEW CLOSE DOUBLE STARS

Identifier	Coordinates RA & DEC (2000)	Flux m_V	Epoch 2016+	Fil.	θ (°)	ρ ($''$)
TYC 416 − 564 − 1	17 45 54.92 +01 34 56.60	10.96	0.4893	I	349.4 ± 0.3	0.490 ± 0.008
TYC 420 − 1003 − 1	17 46 16.60 +01 56 45.87	11.35	0.4893	I	265.4 ± 0.4	0.276 ± 0.009
TYC 416 − 174 − 1	17 46 21.64 +01 22 08.59	10.07	0.4893	I	11.6 ± 0.2	0.613 ± 0.007

format used in the WDS Catalog (Worley & Douglass 1997). The second column gives the official binary star discoverer designation. The third column gives the epoch of the observation in fractional Julian years. The fourth column indicates the filter used. The two following columns contain the measured position angles given in degrees, with the errors of their determination, and the angular separation in arcseconds, with the errors of its determination.

The astrometric measurements of close double stars without known orbits are displayed in Table 2. The symbol (*) indicates that this system was previously discovered but never confirmed. We confirm these systems as double stars. However, for many of them, the current position of the component is far away from the one reported previously. Therefore, it is uncertain to determine whether it is a confirmation or a new pair. The second column gives the

official binary star discoverer designation. The last four columns give the position angle θ (Column 5) with its error $\sigma\theta$ (Column 6) in degrees, and the angular separation ρ (Column 7) with its error $\sigma\rho$ (Column 8) in arcseconds.

Furthermore, we have observed 65 close binary stars with known orbits from the Sixth Catalog of Orbits of Visual Binary Stars (OC6) (Hartkopf et al. 2001). The astrometric measurements are displayed in Table 3. The first 8 columns are the same as in Table 2. The last three columns give the difference between our measurements and the ephemeris calculated for the date of observation, as well as references in the format of OC6. The orbital elements and the complete list of references may be found in the current electronic version of OC6: http://ad.usno.navy.mil/wds/orb6.html.

The last Table 4 displays the astrometric parameters of three new close double stars with separation less than one arcsecond.

The astrometric results include errors arising in the process of recovering the component positions from the power spectrum. In addition, the position angle measure (θ) can have a systematic error of 0.14° and the separation measure (ρ) has an additional error pertaining to the pixel scale.

5. CONCLUSIONS

We present results of double star speckle interferometric observations focused on close binaries from the WDS catalog. We present the astrometric results for 468 resolved stars. We confirm 59 stars as doubles.

For astrometric measurements, we calculate the high resolution autocorrelation function in polar coordinates. It allows one to perform astrometric measurements even for a distorted power spectrum. The coordinates of the global maximum of ACF_p corresponds to the ρ and θ of the component. The measurements can be carried out without a speckle interferometric transfer function correction, because we exclude atmospheric distortion by using the window $W(r, \phi)$. Finally, the self-calibrating shift-and-add technique solves the 180 degree ambiguity.

This research is supported by the Dirección General de Asuntos del Personal Académico (UNAM, México) under project IN107818. Based upon observations acquired at the Observatorio Astronómico Nacional in the Sierra San Pedro Mártir (OAN-SPM), Baja California, México. We thank the daytime and night support staff at the OAN-SPM for facilitating and helping us to obtain our observations. We have made an extensive use of the SIMBAD and ADS services, for which we are thankful. Also, we would like to thank the reviewers for the time they spent on our manuscript and for their comments which helped us to improve it.

REFERENCES

Christou, J. C., Hege, E. K., Freeman, J. D., & Ribak, E. 1986, JOSAA, 3, 204

Guerrero, C. A., Rosales-Ortega, F. F., Escobedo, G., et al. 2020, MNRAS, 495, 806

Hartkopf, W. I., Mason, B. D., & Worley, C. E. 2001, AJ, 122, 3472

Hartkopf, W. I., McAlister, H. A., & Mason, B. D. 2001, AJ, 122, 3480

Kerp, J., Barth, W., Hofmann, K., Reinheimer, T., & Weigelt, G. 1992, ESO Conference on High-Resolution Imaging by Interferometry II. Part 1: ground interferometry and infrared wavelengths, ed. J. M. Beckers & F. Merkle , 1, 269

Labeyrie, A. 1970, A&A, 6, 85

Mitrofanova, A., Dyachenko, V., Beskakotov, A., et al. 2020, AJ, 159, 266

Orlov, V. G., Voitsekhovich, V. V., Mendoza-Valencia, G. A., et al. 2009, RMxAA, 45, 155

Tokovinin, A., Mason, B. D., & Hartkopf, W. I. 2010, AJ, 139, 743

Tokovinin, A., Mason, B. D., Hartkopf, W. I., Mendez, R. A., & Horch, E. P. 2015, AJ, 150, 50

Tokovinin, A., Mason, B. D., Mendez, R. A., Costa, E., & Horch, E. P. 2020, AJ, 160, 7

Worley, C. E. & Douglass, G. G. 1997, A&AS, 125, 523

V. G. Orlov: Instituto de Astronomía, Universidad Nacional Autónoma de México, Apdo. Postal 70-264, Cd. Universitaria, 04510 Ciudad de México, México (orlov@astro.unam.mx).